Journal of Bio- and Tribo-Corrosion (2025) 11:109
https://doi.org/10.1007/s40735-025-01030-8

Synthesis of Aluminium-Ceramic Composites: Mechanical-Wear Characterization of Al7085 – B_4C Micro Composites

M. Hemanth Kumar[1] · R. Saravanan[1] · B. K. Naveen Kumar[2] · Raman Kumar[3,4] · T. Hemanth Raju[5] · A. Bhowmik[6,7] · Madeva Nagaral[8] · Rashmi P. Shetty[9]

Received: 15 February 2025 / Revised: 24 July 2025 / Accepted: 24 August 2025

Abstract
This study investigates the result of incorporating 10 micron-sized B_4C on the wear and mechanical characteristics of Al7085 alloy. Composites with 4, 8, and 12 wt.% B_4C were made by means of stir casting techniques. Always, it is very difficult to have the proper wettability between the metal matrix and carbide particles. In the present research to improve the wettability a halide salt K_2TiF_6 is used. Microstructural analysis utilizing SEM and EDS verified a consistent dispersal of B_4C particles through the Al7085 matrix. The incorporation of B_4C led to notable enhancements in hardness, tensile strength, and compressive strength; however, a decrease in ductility was noted. The improvements in the ultimate strength and hardness of Al70785 alloy with 12 wt.% of 10 micron-sized B_4C is 35.3 and 48%, respectively. Wear tests conducted with varying loads and speeds indicated superior wear resistance in the composites relative to the unreinforced alloy. Scanning electron microscopy examinations of the worn surfaces indicated clear crack and wear contrivances in the Al7085-B_4C composites.

Keywords Al7085 Alloy · B_4C · Tensile properties · Wear · Fractography · Wear debris

1 Introduction

Aluminum metal matrix composites (AMMCs) are gaining recognition as a crucial category of materials in industries including aerospace, transportation, and defence. Their enhanced specific strength, wear resistance provide significant advantages compared to conventional unreinforced materials [1, 2]. The relationship that exists among the aluminium matrix and the reinforcement material is a crucial element affecting the mechanical properties of Al-based MMCs. This bond allows for the reinforcement and matrix to transfer loads efficiently, thus improving the overall mechanical act of the composite [3, 4].

The integration of sustenance material into the alloy enhances properties like as hardness, rigidity, and resistance to wear, creep resistance, and fatigue performance when connected to conventional engineering materials [5]. Previous studies disclose that the utilization of consistent fiber reinforced metal composites has been stuck by elevated. Recently, particulate MMCs have been employed in several construction applications due to their ease of formability and very modest cost. Particulates reinforced composites are utilized effectively in various sectors, including aerospace, automotive, mechanical assemblies, braking systems

✉ Madeva Nagaral
madev.nagaral@gmail.com

1 Department of Mechanical Engineering, University Visvesvaraya College of Engineering, Bangalore University, Bangalore, Karnataka 560001, India

2 Department of Mechanical Engineering, M S Ramaiah Institute of Technology, Bengaluru, India

3 Department of Mechanical and Production Engineering, Guru Nanak Dev Engineering College, Ludhiana, Punjab 141006, India

4 Jadara University Research Center, Irbid 733, Jordan

5 Department of Mechanical Engineering, New Horizon College of Engineering, Bangalore, Karnataka 560001, India

6 Department of Mechanical Engineering Graphic Era (Deemed to Be University), Dehradun 248002, India

7 Centre for Research Impact and Outcome, Chitkara University Institute of Engineering and Technology, Chitakara University, Rajpura, Punjab 140401, India

8 Aircraft Research and Design Centre, HAL, Bangalore, Karnataka 560037, India

9 Mechanical Engineering Department, Nitte (Deemed to Be University, NMAM Institute of Technology (NMAMIT), Udupi, Karnataka, India

Published online: 04 September 2025

for trains and vehicles, military aircraft and related applications [6, 7].

A variety of altered kinds of particulate fortifications as Al_2O_3, SiC, TiC, ZrO_2, B_4C, and Fly Ash [8, 9], are combined with aluminium in order to provide the most effective wear resistance, in addition to the stiffness and specified strengths. As an outcome of its high modulus and strength, in addition to its ceramic particles exhibit strong ability to withstand heat stress and are extensively utilized as support in various developing materials. A growth in the quantity of particles that were present in the aluminium amalgam led to an improvement in the composites'stiffness. B_4C helps metal composites made of aluminium and boron carbide to have better hardness and wear resistance since it serves as a lubricating coating on the contact surface. Additionally, it agrees with minimal heated extension. B_4C contributes to the development of the material's hardness, wear resistance, and mechanical qualities when subjected to high temperatures through its use. The high specific quality and strength of aluminium metal composites, in count to their excellent wear resistance, are the primary factors for their existence utilized in the aviation and car industries [10]. Shorowordi et al. [11] studied the interface characteristics of SiC, B_4C and Al_2O_3 reinforced Al composites developed by stir method. Al-SiC interface was obtained at processing time of 30 min. Fractured surfaces of Al-B_4C composites shown a better bonding compared to Al-SiC and Al-Al_2O_3 composites.

Aluminium composites largely rely on the preparation method; therefore, the selection of the production method plays a crucial role in meeting mechanical requirements and providing functional properties [12, 13]. The challenges associated with delivering aluminium composites generally include the elevated costs of the supporting materials, the non-homogeneous or heterogeneous distribution of reinforcements within the matrix, and, in some instances, higher investment costs. The strategic approach to assembling expanding their usage are dependent on composites [14]. The fundamental methods of manufacturing employed mass metal composites comprise powder metallurgy, compo casting, infiltration, and stir casting. [15]. Mehmet et al. [16] synthesized the TiO_2 and Kaoline reinforced Al7075 alloy hybrid composites. The prepared hybrid composites were exhibited the higher micro-hardness and improved tribological properties.

Several aluminium alloys like Al1100, Al2024, Al5052, Al6061 and Al7075 are available for industrial applications. In the present research 7XXX series aluminium alloy Al7085 has been selected, the reason is to develop the alternate material for the Al7075 alloy, especially for the aerospace applications. This endeavor involves the utilization of a distinctive two-stage reinforcement count technique to incorporate 4, 8, and 12 wt.% of 10 micron-sized B_4C particles into Al7085 alloy composites. To prepare the metal matrix composites usually ceramic reinforcements in the form of oxides, nitrides and carbides are used. The maximum 15 weight percentage of reinforcement can be used to synthesize the metal base composites, beyond this is very difficult to have good wettability between the matrix and reinforcement. So, one can use any combination of weight percentage below the 15 wt.% to fabricate the composites, it may be 4, 8 and 12 or 5, 10 and 15 or 3, 6, 9 and 12. In the present study, it is considered 4 to 12 wt.% in steps of 4 wt. In this investigated the mechanical and wear possessions of the Al7085 alloy with 10 micron-sized B_4C composites.

2 Experimental Details

2.1 Materials Used

Metal composites comprising 4, 8, and 12 wt.% of B_4C particulates, each with a size of 10 microns, were fabricated using the stir casting method. The production of MMCs involved the utilization of an Al7085 alloy as the primary material, complemented by B_4C particles measuring 10 µm, which served as reinforcements. Figure 1 shows the micrograph of B_4C particles used in the study. Al7085 alloy chemistry is presented in Table 1.

2.2 Preparation of Composites and Testing

The manufacturing process for Al7085 alloy reinforced with B_4C composites utilizes a liquid metallurgy method based on stir casting technique. Al7085 ingots with a specified weight are positioned and heated in an electric furnace until they reach the molten metal phase. Aluminium alloy typically

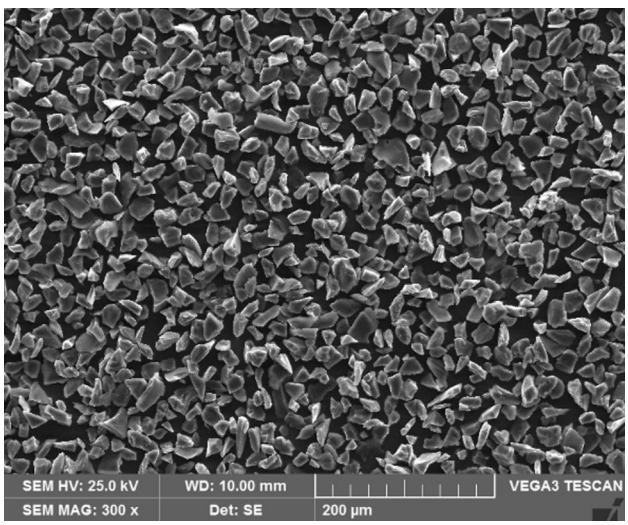

Fig. 1 SEM of 10 micron size B_4C particles

Table 1 Chemistry of Al7085 alloy by weight %

Zn	Mg	Si	Fe	Cu	Ti	Mn	Cr	Al
8.5	1.80	0.05	0.08	1.90	0.06	0.04	0.04	Balance

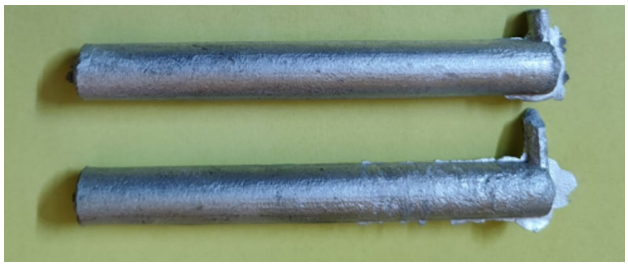

Fig. 2 Prepared Al7085 alloy B_4C composite

Fig. 3 Tensile test specimen

begins to melt at 660 °C; however, the metal is subsequently superheated to a temperature of 750 °C. Thermocouples suitable for the specific temperature range are employed to measure and record the melting and superheated temperatures. Hexachloroethane (C_2Cl_6) [17, 18] is utilized to degas molten metal in the crucible for around three minutes. A steel rotor with blades, affixed to a shaft stirrer and covered with zirconia is employed for agitating molten material. The agitator is submerged in the molten Al7085 to a depth of roughly 65% within the crucible. Agitation of the molten metal is accomplished by rotating the stirrer at around 300 rpm, leading to vortex formation. During the stirring of molten metal, B_4C particulates with K_2TiF_6 halide salt, constituting 4 wt.% of the charged Al7085 alloy, should be preheated separately to 300 °C before being gradually introduced into the molten metal vortex in stages. The stirring process continues until complete wettability is achieved between the Al7085 alloy matrix and B_4C reinforcing particulates, thereby establishing interfacial shear strength. The cast iron molds are filled with matrix and B_4C measuring a length of 120 mm and 15 mm in diameter, resulting in an Al7085 alloy composite containing 4 wt.% of B_4C. The same method is utilised for the production of composites containing B_4C particulates at varying weight percentages. Figure 2 illustrates the prepared composites of Al7085 with B_4C.

Following the casting process, the specimen undergoes preparation for micro-structural analysis with scanning electron microscope to evaluate the consistent reinforcement dispersal particulates within the Al7085 alloy. Micro-graphs of the microstructure are captured for Al7085 alloy and for Al7085 alloy with varying amounts of weight of B_4C composites. The dimensions of the specimen for microstructure analysis are with diameter of 15 mm and 5 mm in depth. The surface of the specimen is polished using 240 to 800 grit. The specimen is then refined using polishing paper to achieve an enhanced smooth finish on the polishing machine. Subsequently, the specimens undergo a cleaning process using distilled water to diminish any foreign particles, such as dirt and additional possible contaminants that could exist on the specimen. Further, the specimens are treated with Keller's reagent for etching [19, 20].

This study examined densities of Al7085 alloy reinforced with B_4C composites. The experimental densities were assessed employing the usual weight method, whereas the theoretical values were computed utilising the law of mixtures. According to ASTM E10 [21], the example is suitably prepared for the hardness test. Hardness is assessed via a Brinell hardness testing apparatus. The specimen's surface has a sleek, polished appearance. A ball depression of 5 mm has been documented, with a stress of 250 kg exerted on the specimen. Three readings are documented, and the average outcomes are assessed.

The samplings are fabricated in accordance with ASTM E8 [22, 23] to evaluate the tensile characteristics of as cast Al7085 with differing weights of B_4C particulate-reinforced composites as shown in Fig. 3, the sample has dimensions of 104 mm in length and 9 mm in gauge diameter. The computer-controlled INSTRON tensile machine is employed to evaluate tensile strength, analyse uniform distribution effects, and investigate the behaviour of Al7085 reinforced with B_4C composites under unidirectional tension. This tensile test is accompanied to know the ultimate strength, yield strength, and ductility. The compressive strength is assessed in accordance with the ASTM E9 standard.

The pin-on-disc device was employed to analyze the wear behavior of Al7085 and Al7085 with B_4C reinforced composites. The investigations were conducted in harmony with the ASTM G-99 [24, 25] on an 8 mm measurement and a 30 mm length example, as illustrated in Fig. 4. After conducting studies on the direction of dry sliding wear, the wear was determined at a sliding velocity of 2.82 m/sec over a distance of 2000 m, with applied loads of 9.8 to 39.2 N in steps of 9.8 N. The wear behaviour of Al7085 composite materials was examined at sliding speeds of 1.4 m/sec to

Fig. 4 Wear test specimen

Fig. 5 Ducom made pin-on-disc wear test apparatus

2.8 m/sec, under a load of 39.2 N and a sliding distance of 2000 m.

Debris from wearables was gathered during the wear experiments conducted with the pin-on disc instrument. This debris was then employed to investigate various wear mechanisms by SEM micrographs. Additionally, micrographs were employed to investigate the wear morphology of the Al7085 and the Al7085 with B_4C composites in order to ascertain the distinct wear behavior. Figure 4 represents the wear test specimen. Figure 5 is demonstrating the Ducom made pin-on-disc wear apparatus.

3 Results and Discussion

3.1 Microstructural Behavior

Figure 6a–d displays the SEM micrographs of the Al7085 and the Al7085 infused by 4, 8, and 12 wt.% of B_4C composites. Figure 6a displays the SEM picture of the Al7085 alloy. In the absence of particles, this reveals distinct grain boundaries. The image is free of any casting flaws. Figure 6b–d displays the Al7085 composites containing 4 to12 wt.% B_4C, respectively. The micrographs clearly demonstrate that the B_4C reinforced composites contain visible micro particles. The composites exhibit a superior distribution of carbide particles, attributed to the innovative 2-step casting process utilized in the synthesis of the composites. Additionally, the microstructure surface of Al7085 alloy containing 12 wt.% of B_4C composites exhibits a higher density of particles, which are consistently dispersed across the matrix surface. Always it is a challenging process to have the strong bonding between the metal matrix and ceramic reinforcements. In the present research for every 1 g of reinforcement 0.20 g of K_2TiF_6 is added. This K_2TiF_6 acts as bonding agent between the matrix Al7085 alloy and B_4C particles by forming an interfacial layer of Ti. In the Fig. 6b–d it is clear visibility of Ti layer formed between the carbide particles and matrix. The enhancement in properties of Al7085 alloy is due to this strong wettability process.

EDS analysis is conducted on the Al7085 alloy with 4, 8, and 12 wt.% B_4C composites. Figure 7a presents the EDS pattern of the Al7085 alloy, which primarily comprises Zn, Mg, and Cu as its major alloying elements. Additionally, Fig. 7b–d presents the EDS spectra of Al7085 alloy containing 4, 8, and 12 wt.% of B_4C composites.

3.2 Density Measurements

B_4C particle-reinforced composites and composites composed of Al7085 alloy with 4, 8, and 12 weight percent of B_4C particles have different densities, as shown in Fig. 8. Applying the mixture rule allows for the theoretical computation of the densities of both the Al7085 and the B_4C composites. In addition, using the weight notion as a guide, experimental densities are effectively calculated. B_4C particles utilized in the research have a density of 2.52 g/cc, this is inferior than the density of Al7085 alloy, which is 2.82 g/cc. Aa in Fig. 8, the density of the Al7085 has dropped from 2.82 g/cc to 2.78 g/cc when the weight percentage of B_4C in the Al7085 matrix increases from 4 to 12 wt.%. This decreased density is owing to the lower B_4C particle density in relation to the Al matrix density [26]. This lowered density is an outcome of the inclusion of B_4C particles. The reduced density of the reinforced particles results in a decline in the matrix's overall density. Additionally, the graph shows that the difference between the two densities is not very large and that the experimental density is somewhat lower than the theoretical densities. The importance of the casting process used to manufacture composites is demonstrated by the link between the observed density of the Al7085 alloy (2.750 g/cc) and the theoretical density of the Al7085 matrix (2.82 g/cc). Density is the major parameter in the design and development of any aerospace components. In the present study boron carbide particles are used to prepare the Al7085 alloy composites. These particles density is slightly lower than the Al matrix. For the aerospace

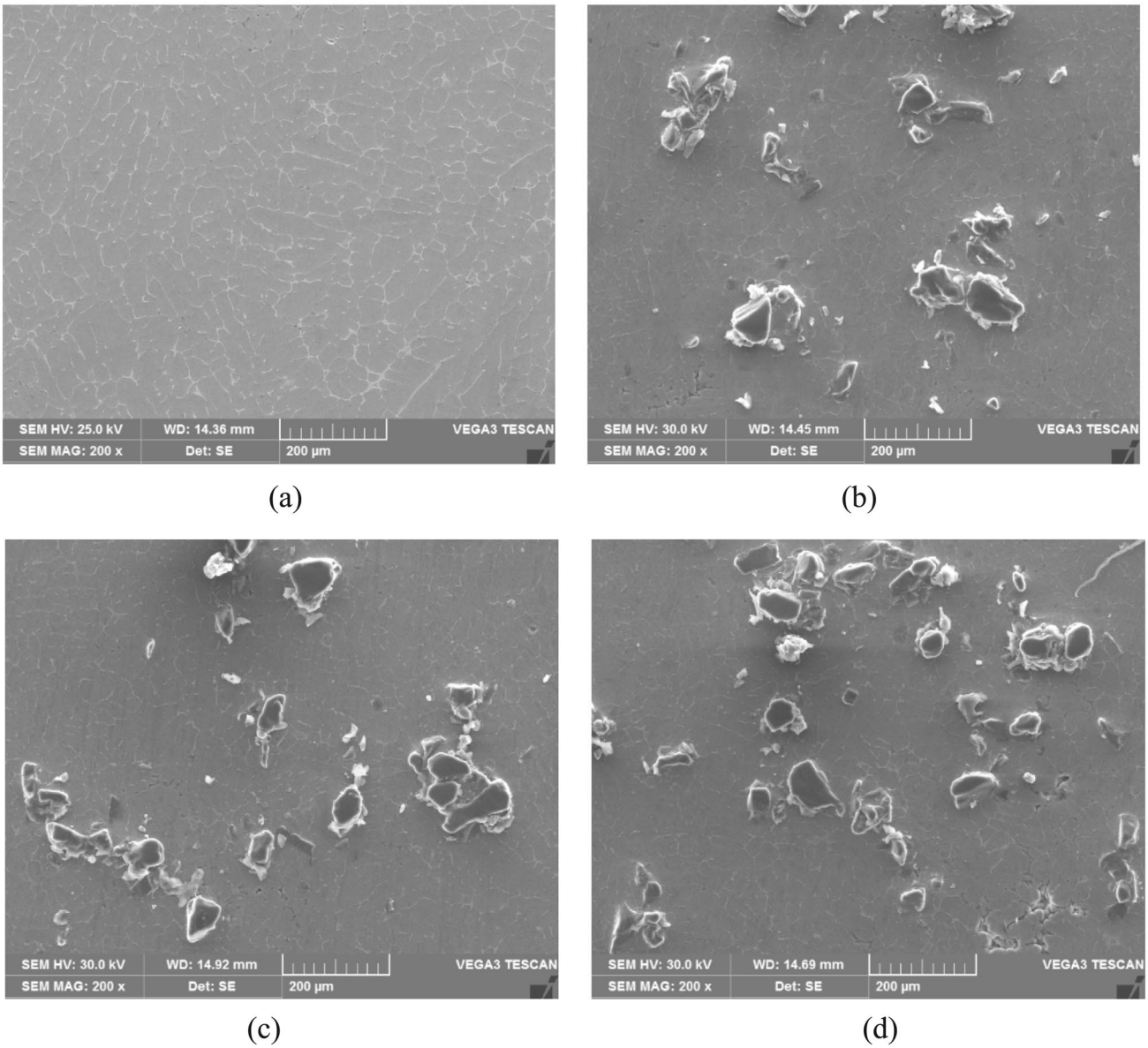

Fig. 6 SEM micrographs of **a** Al7085 **b** Al7085-4 wt.% B_4C **c** Al7085-8 wt.% B_4C **d** Al7085-12 wt.% B_4C

applications the decrease in density helps in reducing the weight of the component. Since, in the present research Al-B_4C composites exhibited superior properties with decrease in the density, hence structural integrity remains un-affected.

3.3 Hardness Measurements

The hardness of Al7085 and Al7085 augmented with B_4C micro particles composites is confirmed in Fig. 9. The graph shows that a rise in the B_4C particle weight percentage from 4 to 12 wt.% in Al7085 alloy correlates with an enrichment in the hardness of the Al7085. The hardness of Al7085 is measured at 67.9 BHN. Following the combination of 4 wt.% of B_4C particles, the hardness increases to 79.1 BHN. The hardness of Al7085 containing 12 wt.% of B_4C measures 100.5 BHN. This increased hardness is primarily attributed to the higher quantity of hard B_4C particles present. The rise in hardness is attributed to the existence of micro particles, which affect the grain magnitude of the filler, subsequently influencing the grain size of the composite [27]. Topcu et al. [28] developed 5 to 20 wt.% of B_4C reinforced composites. The Al-B_4C composites were found with higher hardness as wt.% of carbide particles increased in the matrix. Further, the increase in the hardness of Al-B_4C composites were observed by the Mehmet and co-authors [29].

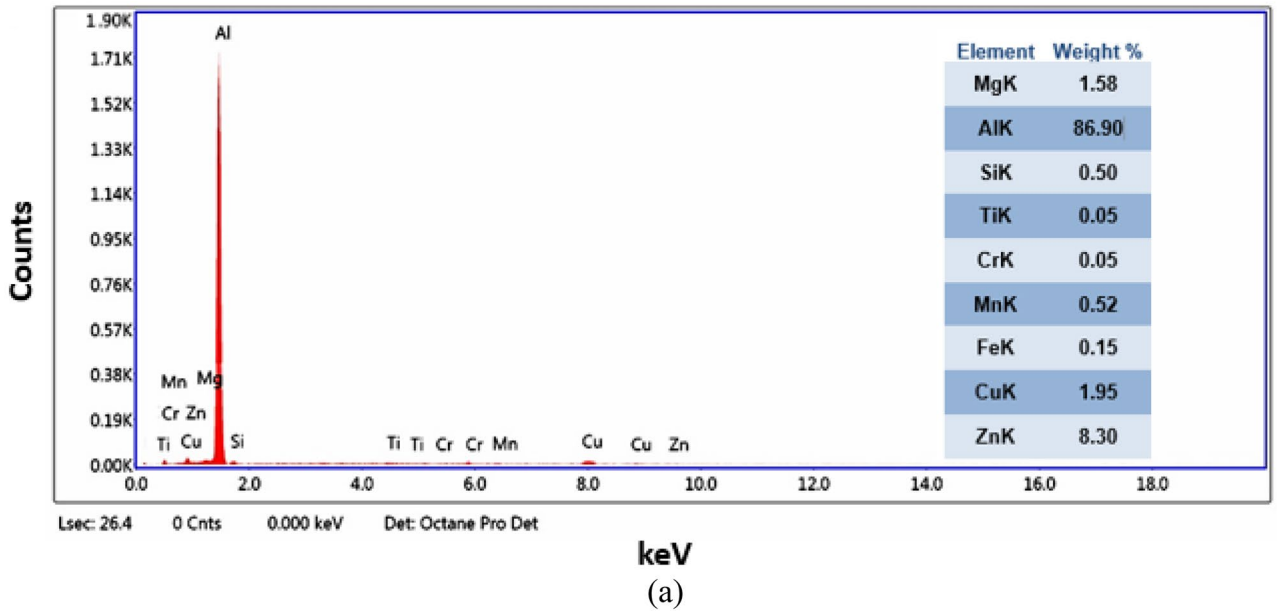

Fig. 7 EDS spectrums of **a** Al7085 **b** Al7085-4 wt.% B_4C **c** Al7085-8 wt.% B_4C **d** Al7085-12 wt.% B_4C composites

3.4 Ultimate and Yield Strength

Figures 10 and 11 depict the influence of B_4C on the ultimate and yield strength of the Al7085, respectively. The use of B_4C particles has improved the tensile strength of Al7085. The ultimate and yield strength of Al7085 are 212 MPa and 181.5 MPa, respectively. The ultimate and yield strengths of Al7085 with 12 wt.% B_4C particle composites are 286.8 MPa and 253.2 MPa, respectively. The strength of Al7085 alloy escalates with the weight percentage of B_4C, increasing from 4 to 12%. The incorporation of B_4C particles augments the strength of the parent Al7085 alloy. The enrichment of strength in the Al7085 composite is ascribed to the thermal expansion discrepancy between B_4C and the aluminium lattice.

The addition of B_4C elevates the dislocation density in the lattice material, acting as a strengthening mechanism for the Al matrix. The augmentation of dislocation density further elevates the strength of the Al7085 alloy with B_4C composites. B_4C's presence near the grain boundary of the Al7085 matrix effectively inhibits particle migration across the grain boundary, enhances the boundary's ability

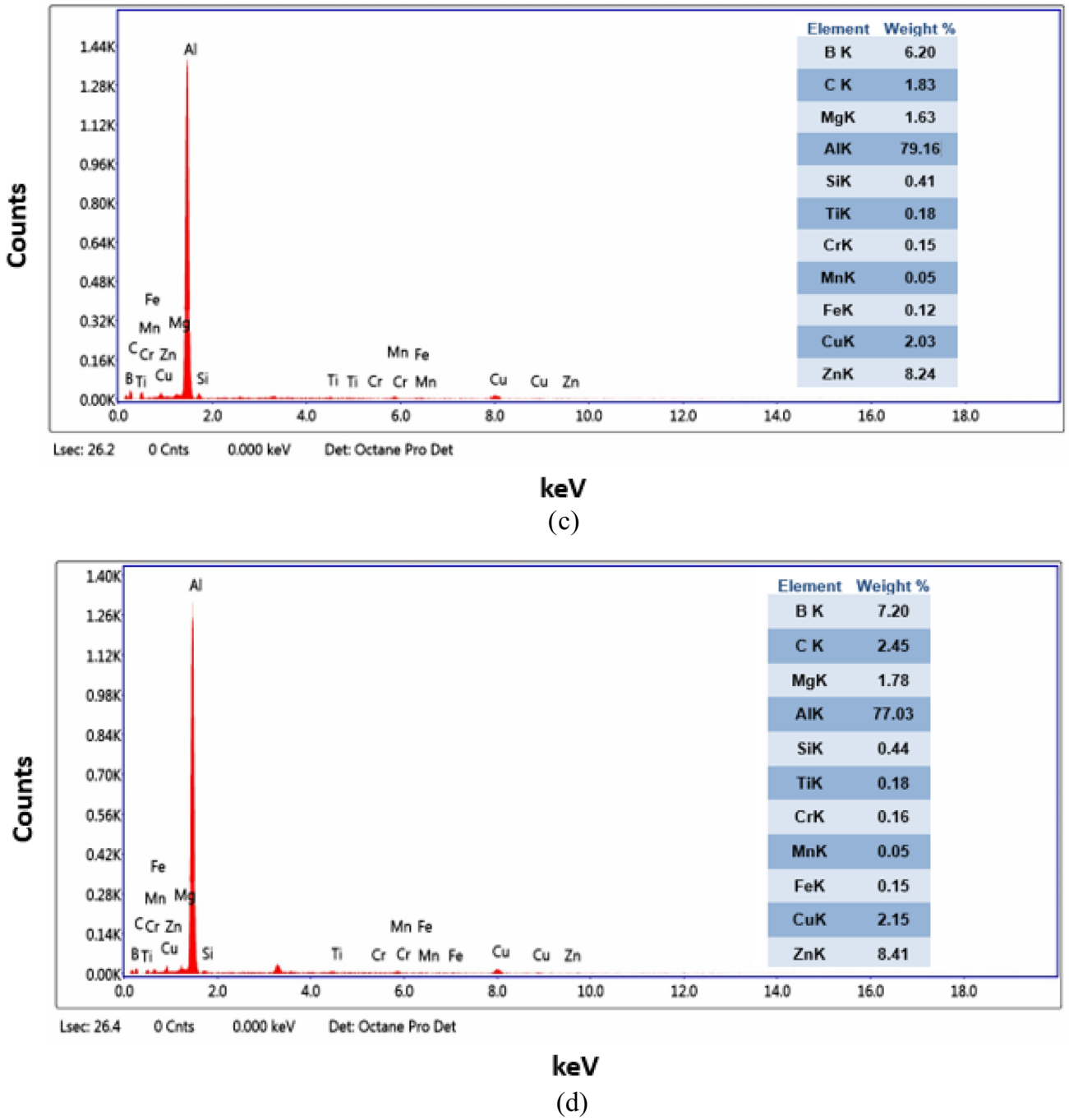

Fig. 7 (continued)

to prevent separation growth, and reinforces the matrix, thereby improving the composite strength. The improved tensile strength was found by the results of Al7075-B_4C composites by Mehmet et al. [30].

Incorporating B_4C reinforcement particles into composites increases their yield strength, and this study looks at how different strengthening procedures affect that increase. This is accomplished by merging the ideas of continuum mechanics reinforcement with micromechanics. The investigation into the effects of increasing the reinforcing quantity in Al7085 on different strengthening methods was carried out in tandem with the analysis. According to continuum mechanics, the load can be transferred from the malleable matrix to the stiff ceramic reinforcing particle by a strong adhesion at the particle–matrix contact. The inclusion of strong reinforcing particles within the matrix is responsible

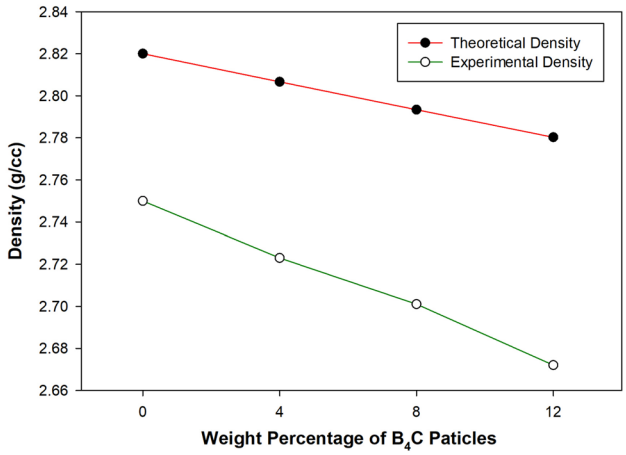

Fig. 8 Densities of Al7085 with B_4C composites

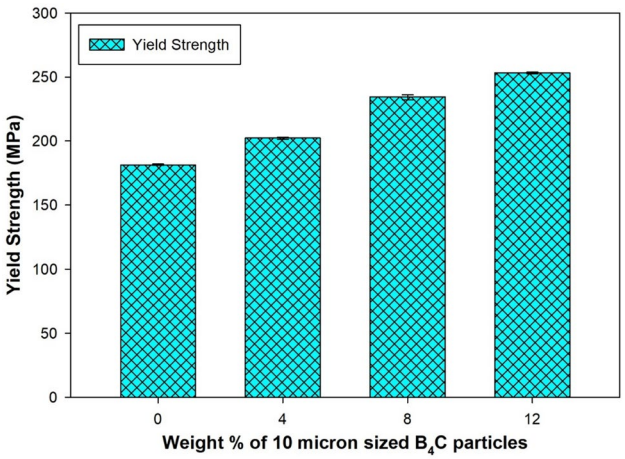

Fig. 11 Yield strength of Al7085 alloy with B_4C composites

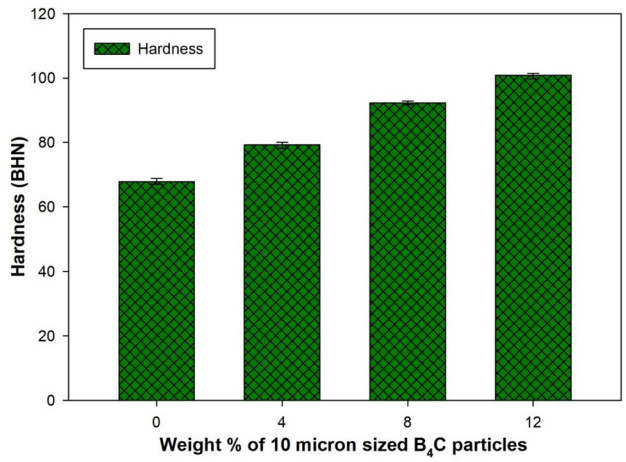

Fig. 9 Hardness of Al7085 alloy with B_4C composites

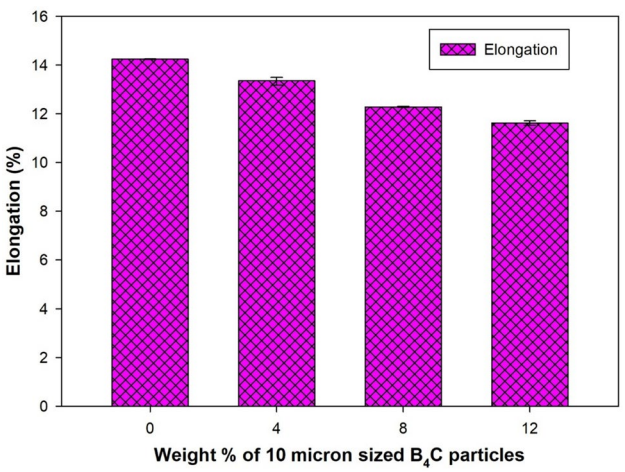

Fig. 12 Percentage elongation of Al7085 alloy with 10 micron-sized B_4C composites

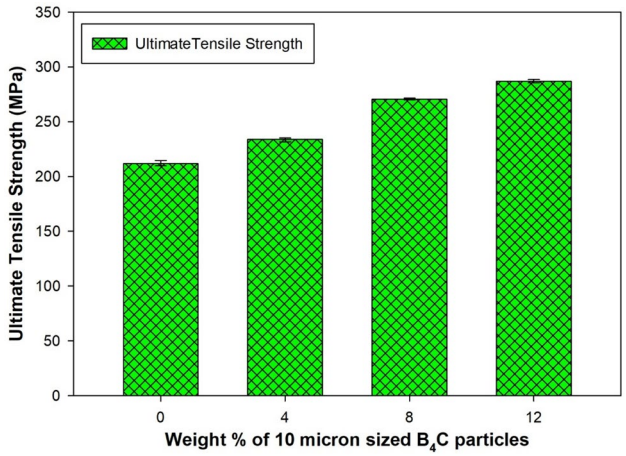

Fig. 10 Ultimate strength of Al7085 with B_4C composites

for the composite's improved strength. There are various strengthening mechanisms which affect the strength parameters of metal composites like i) Load transfer mechanism like continuum mechanics ii) Micro-mechanics strengthening iii) Grain refinement strengthening like Hall-Patch effect iv) Orowan strengthening.

3.5 Percentage Elongation

On display in Fig. 12 is the impact that B_4C particles with a size of 10 microns have on the ductility of the Al7085 alloy. The ductility of the Al7085 alloy decreased consequently influence of B_4C particles and their presence. Because of the occurrence of hard B_4C particles, the ductility of the material has drastically decreased. The ductility deteriorated even further as the weight percentage of B_4C increased to

12 weight percent. During the course of deformation of the Al7085 alloy matrix, these particles serve as a restraint [31].

Figure 13 is depicting stress vs strain plot of the Al7085 alloy and varying wt.% of B_4C reinforced composites. From the plot it is confirmed that as the wt.% of carbide particles increased in the Al7085, there is enhanced stress values with slight decrease in the strain. The increased resistance to deformation is observed, and this phenomenon is due to the strong presence of bonding between the matrix and particles.

3.6 Compression Strength

Figure 14 illustrates the compressive strength of composites made of Al7085 alloy and Al7085 alloy with micro B_4C particulates; both of these composites are available. Evidence indicates that these particles influence the compression behavior of the aluminium alloy. As cast, the Al7085 alloy has a compression strength of 582 MPa, whereas the Al7085-4 wt.% B_4C has a compression strength of 667.7 MPa, the Al7085-8 wt.% B_4C alloy weighs 745.3 MPa, and the Al7085-12 wt.% B_4C alloy weighs 814.8 MPa. The compressive strength of the Al7085 alloy exhibits a 28.5% enhancement because of the addition of 12 weight percent of $_{B4}C$ particles. The compressive strength of the ceramic particles is always an indication of how the particles behave when exposed to compression. The strength of the Al7085 alloy is impaired as a result of these ceramic particles, which have a very high compression strength.

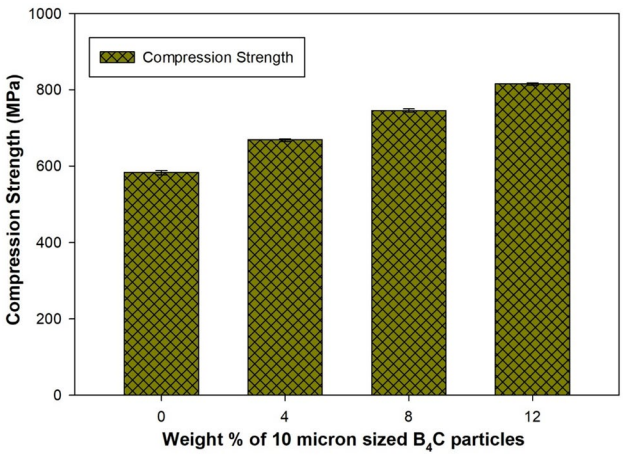

Fig. 14 Compression strength of Al7085 alloy with B_4C composites

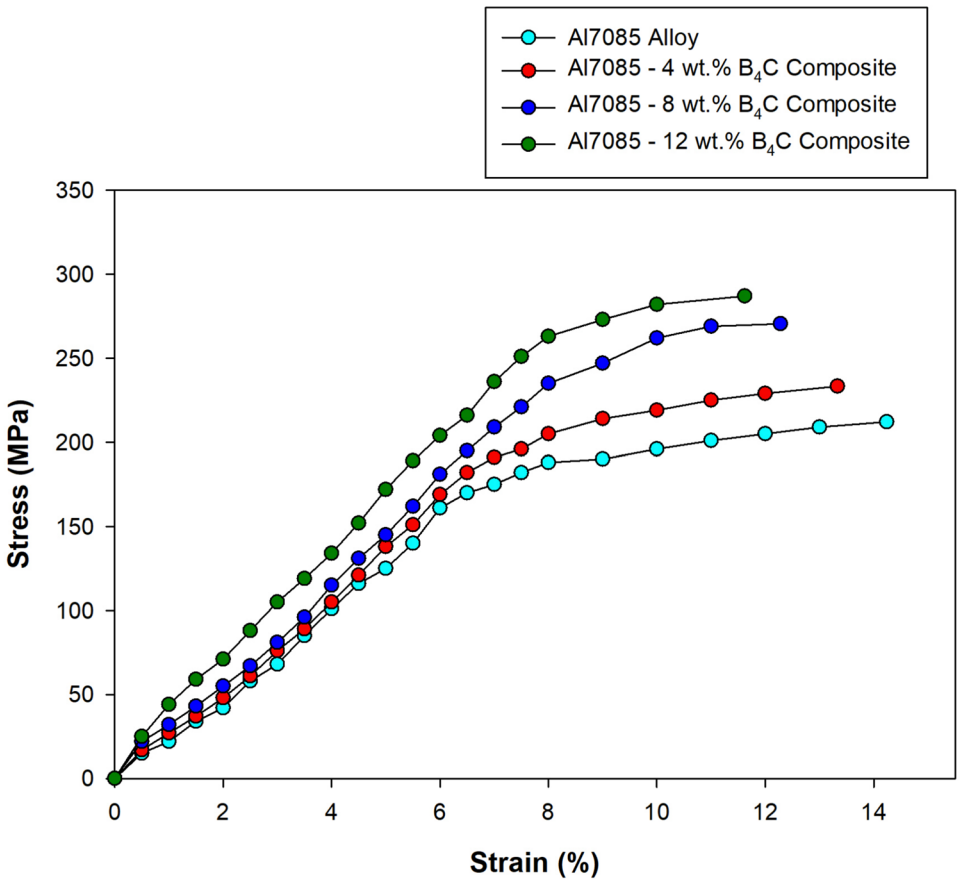

Fig. 13 Stress vs Strain plot of Al7085-B_4C composites

3.7 Tensile Fractography

Exhibited in Fig. 15 is the cracked surface morphology of the Al7085 alloy in addition to its boron carbide composites. Figure 15a shows the fracture morphology of Al7085, which is a plastic fracture morphology. The fracture is a property of the material. Figure 15b–d depicts the fracture profile of an Al7085 alloy that contains 4, 8, and 12 weight percent of B_4C micro composites. Due to the inclusion of the hard particles, the Al/B_4C composites undergo a change in both the size and depth of their dimples. A particular quantity of particles scattered at the dimple's edge as a result of the composites'crack propagating at the contact during the rupture progression [32]. As a result, the dimple developed. Because of the higher percentage of B_4C particles in the matrix, the it shows brittle breakage. This happens when the Al7085 alloy's carbide particle mass fractions have increased. Figure 15a describes the ductile mode of fracture, further Fig. 15b–d are showing brittle fracture mechanisms.

3.8 Wear Properties

The wear behavior showed on the Al7085 and B_4C composites at loads alternating from 9.8 N to 39.2 N in 9.8 N

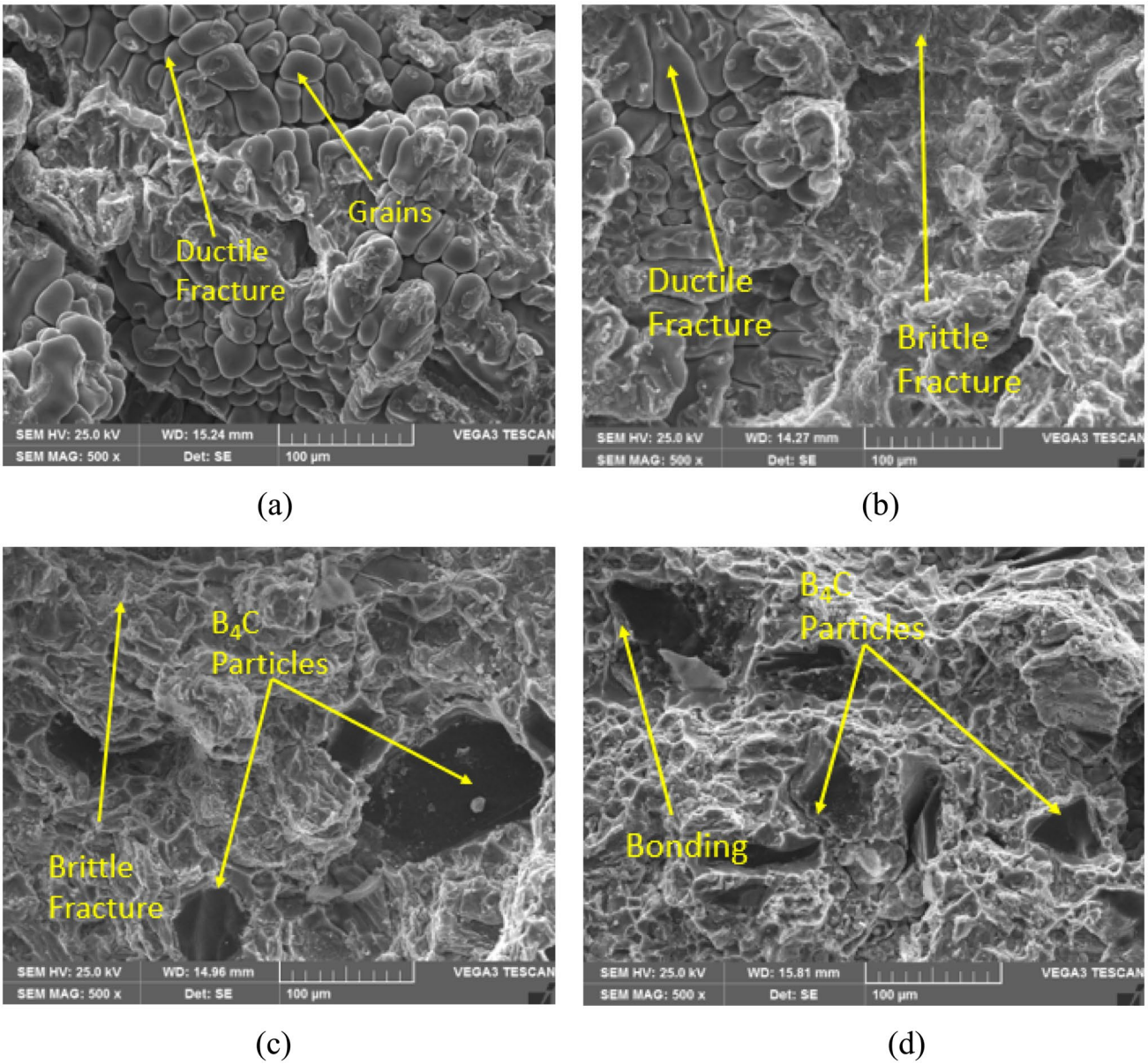

Fig. 15 Scanning electron micrographs of tensile fractured surfaces of **a** Al7085 alloy **b** Al7085-4 wt.% B_4C **c** Al7085-8 wt.% B_4C **d** Al7085-12 wt.% B_4C composites

increments, with a constant speed of 2.8 m/sec and a sliding distance of 2000 m. Correspondingly, research was conducted at sliding speeds ranging from 1.4 m/sec to 2.8 m/sec rpm in 0.45 m/sec increments, with constant 39.2 N weights at a distance of 2000 m. In each and every test, the quantity of wear is represented in microns and is measured in terms of height loss.

The load is a pivotal aspect that significantly influences wear loss. Extensive research has been conducted on the impact of load in wear trials to control the wear of alloys. Furthermore, graphs depicting wear loss in relation to wear rate under various loads of 9.8 N to 39.2 N, maintained at a persistent distance of 2000 m and a sliding speed of 2.8 m/sec, have been constructed to examine the influence of load on wear.

The effects of load on the wear parameters of Al7085 alloy and Al7085 with 4, 8, and 12 weight percent of B_4C reinforced micro composites are shown in Fig. 16. It is evident from graph 16 that when the load increases from 9.8 N to 39.2 N, the wear of all composites and the base Al7085 alloy increases. At a maximum load of 39.2 N, the sliding face's temperature hits the critical limit. Consequently, when the tension on the pin grows, so does the loss of the metal composites and matrix Al7085 alloy. when seen in Fig. 16, the Al7085 alloy when cast shows the maximum attrition loss under all loading situations.

Figure 17 shows that the compounds'wear loss decreases as the weight % of boron carbide in the Al7085 alloy increases. The increased hardness of carbide particles, which prevent wear loss, may be the cause of the Al7085 alloy's increased wear resistance with B_4C reinforced composites as in Fig. 17.

As shown in Fig. 18, the wear misfortune is associated with the deviation of speed for a variety of examination tasks that involve altering arrangements. With a load of 39.2 Newtons, the trial is corresponding with a disc speed that ranges from 1.4 m per second to 2.8 m per second. The assumption that wear misfortune increases with increasing speed is based on the data presented in Fig. 18. When compared to B_4C strengthened metal composites, the influence of sliding velocity is greater as it pertains to the base Al7085 combination. Yahya et al. [33] investigated 15 wt.% of SiC particles on the wear behavior of $Al7SiMg_2$ composites prepared by liquid melt process. The wear resistance of Al alloy was increased due to the increase in the hardness of the composites with the presence of hard SiC particles.

Figure 19 indicates at all sliding velocities, the wear loss of the composites is significantly less than that of the Al7085 alloy, especially when the Al7085 alloy is reinforced with 12 weight percent of 1 micron-sized B_4C particles. As the number of boron carbide particles in the composite increases, the

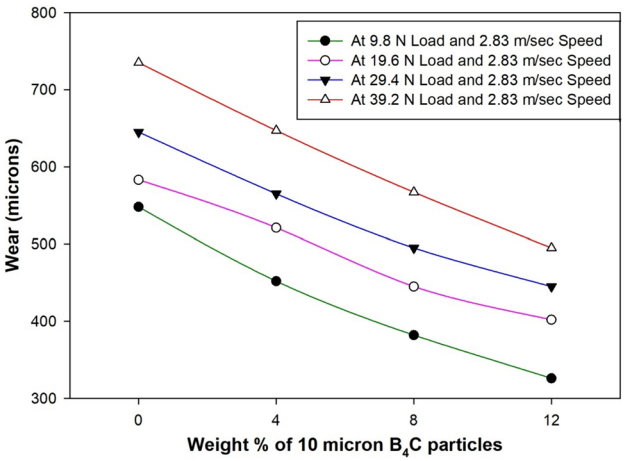

Fig. 17 Wear of Al7085 with varying wt.% 10 micron-sized B_4C composites

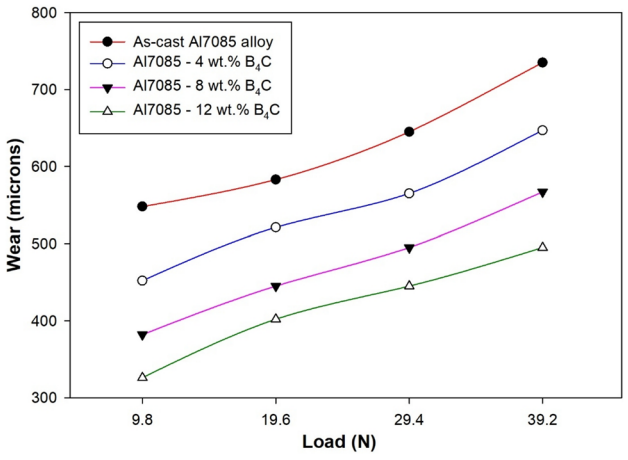

Fig. 16 Wear of Al7085 with B_4C composites at different loads and constant speed

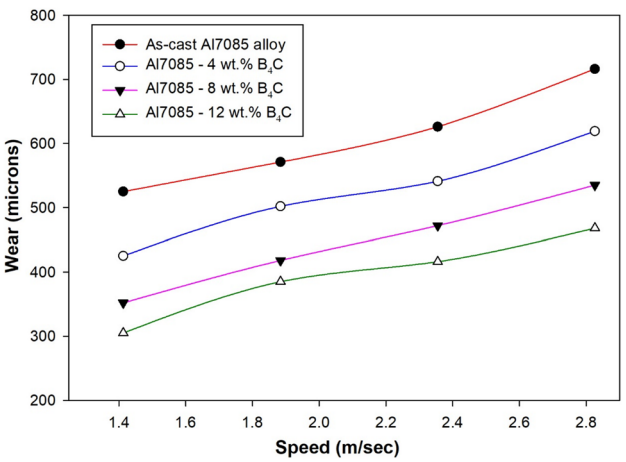

Fig. 18 Wear of Al7085 alloy with 10 micron size B_4C composites

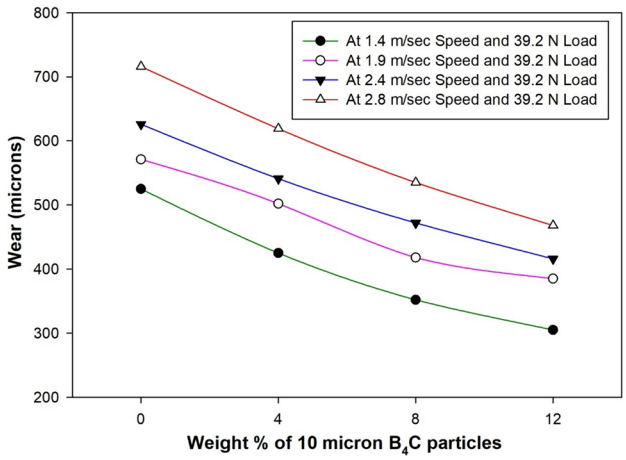

Fig. 19 Wear of Al7085 alloy with varying weight percentages B_4C composites

abrasion losses decrease as in Fig. 19. The current study's results are consistent with those of other researchers who have carried out related investigations [34].

3.8.1 Worn Morphology and Wear Debris

Figure 20a–d represents the worn surfaces morphology various composites studied. Examining the worn morphology of Al7085, along with its composites containing 4 to 12 wt.% of B_4C, is crucial as it reveals the various wear mechanisms experienced by materials of differing compositions. In the process of sliding, the Al7085 alloy matrix exhibits a lower hardness compared to the material of the rubbing disc, leading to a viscid movement of the Al7085 matrix. This phenomenon manifests as the formation of pins that induce plastic deformation on the specimen's surface, ultimately resulting in significant material loss [35, 36]. The surface of Al7085 alloy exhibits grooves, micro-pits, and a fractured oxide layer, as illustrated in Fig. 20a, which likely contributed to the observed growth in wear loss. In the case of Al7085 alloy containing 4, 8, and 12 wt.% of boron carbide composites, the viscous tide of the matrix is notably constrained, as illustrated in Fig. 20b–d. It is evident that the incorporation of carbide particles has led to a reduction in grooves or erosion, indicating an increasing confrontation to wear loss [37–39]. In the meantime, the addition of hard particles appears to shift stress to hard particles, causing strain concentration around these particles and a decrease in fractures and grooves on the worn surface area [40, 41].

Figure 21a depicts a picture of debris that appears as a result of the wear of the Al7085 aluminium alloy at highest load and speed combination. The amount of wear that the Al7085 alloy has experienced can be determined by the size of the debris that is caused by the wear mechanism. The elongated layers formed from the eroded surface could not withstand the substantial load and as a result, the layers were torn and discarded as a slender plate. Figure 21b illustrates wear debris of Al7085 with 12 wt.% of B_4C particles incorporated into the metal composites; the debris appears as fragments crushed between the test specimen and the revolving disc. The wear debris of as cast Al7085 alloy were slightly larger than the Al7085 with 12 wt.% of B_4C reinforced composites. However, some larger debris were observed in the both cases due to plastic deformation and adhesive wear behavior of matrix material. The wear debris of carbide-reinforced composites demonstrates reduced wear with microscopic particles, such as fragments extracted from the pin [42].

4 Conclusions

This study involves the production of Al7085 composites reinforced with alloys with B_4C particles of 10 microns in size, utilising the stir technique while varying the B_4C content at 4, 8, and 12 wt.%. Density, hardness, tensile strength, compression properties, and dry sliding wear characteristics of the metal alloy Al7085 composites were analyzed. The composite or framework exhibits a pore-free structure and a consistent distribution of tiny particles, as evidenced by SEM microphotographs. When compared to the parent Al7085 alloy, the reinforced composites with B_4C particles showed improved hardness, tensile strength, and compression strength. The ultimate strength of the Al7085 alloy was increased by 26%, hardness by 32.4% and the compression strength was enhanced by 28.5%. The density of the metal composites was somewhat lower than that of the Al7085 alloy. Both brittle and ductile fracture mechanisms can be seen in a tension broken surfaces. The wear resistance of the cast alloy Al7085 was enhanced by the inclusion of 10 micron-sized particles. Both sliding speed and applied load had an impact on the wear behaviour of Al7085 alloy and its composites. The wear loss of Al7085 metal and its composites with boron carbide particles increased in tandem with the rise in load and speed. Improved wear confrontation is shown by the SEM images of worn surfaces and wear debris. The present research is to develop the alternate materials for Al7xxx series Aluminium alloys which are widely used for static load carrying applications in the aerospace components like wing root fittings, vertical tail mounting brackets, landing gear attachment and other backstories. With the incorporation of B_4C particles, the strength improvement is in the range of 35 to 40%. This enhancement in strength will further helps in designing the aerospace components with reduced cross-sectional area, which helps in decreasing the weight of the component.

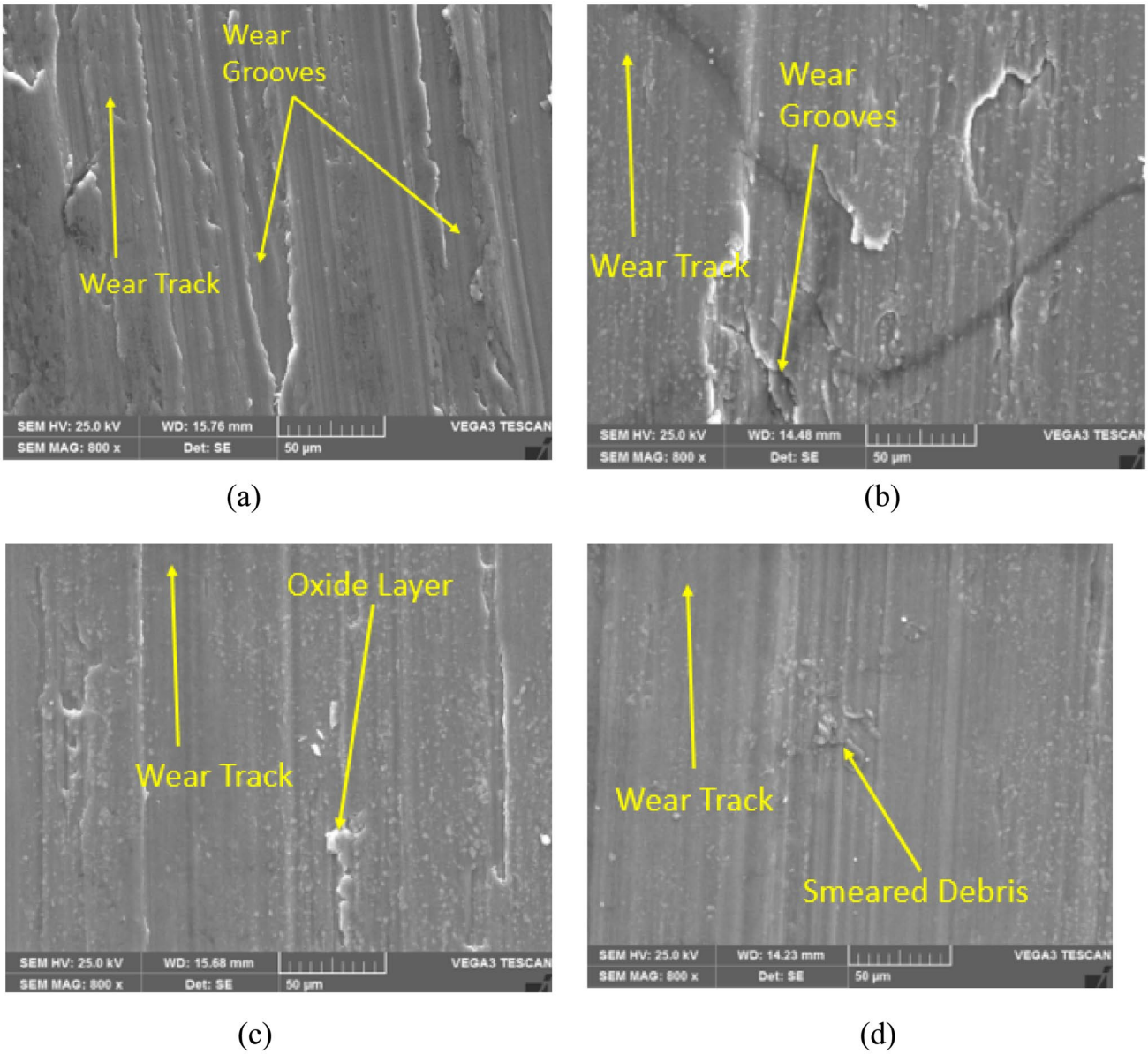

Fig. 20 SEM micrographs of worn surfaces of **a** Al7085 alloy **b** Al7085-4 wt.% B_4C **c** Al7085-8 wt.% B_4C **d** Al7085-12 wt.% B_4C composites

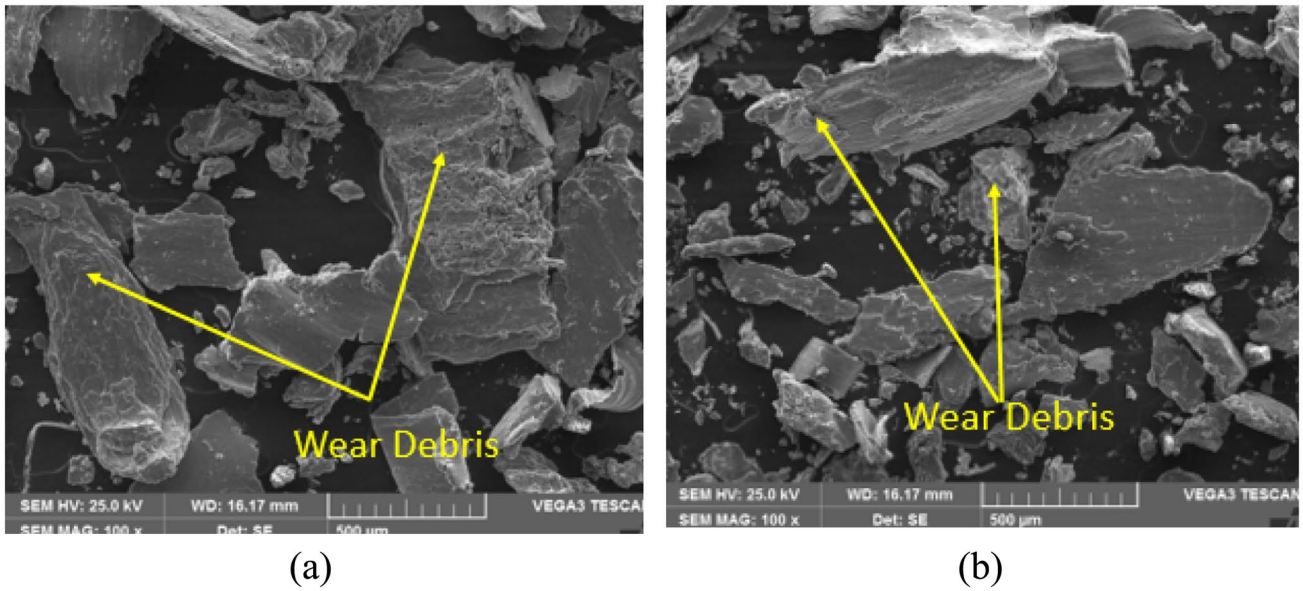

Fig. 21 SEM micrographs of wear debris of **a** as cast 7085 alloy **b** Al7085 alloy with 12 wt.% of B_4C composites

Author Contributions HKM and RS Drafted the manuscript, NKBK and RK Results and Discussions, HRT and AB Corrections, MN Corrections, RP Drafting and Results.

Funding No Funding.

Data Availability No datasets were generated or analysed during the current study.

Declarations

Conflict of interest The authors declare no competing interests.

References

1. Nithin BN, Vishwanath KC, Yadav SM, Namdev N, Shetty S, Nagaral M (2024) Microstructural and tensile characterisation of Si_3N_4 reinforced Al2219 alloy composites. J Mines Met Fuels 72(12):1361–1369
2. Nithin BN, Nagaral M, Maiyya M, Nalband F, Auradi V (2024) Mechanical properties of ZrO2 particles reinforced Al2219 alloy metal composites prepared by stir casting process. J Mines, Metals & Fuels 72(9):937
3. Ali Z, Muthuraman V, Rathnakumar P, Gurusamy P, Nagaral M (2022) Studies on mechanical properties of 3 wt% of 40 and 90 µm size B_4C particulates reinforced A356 alloy composites. Mater Today Proc 52:494–499
4. Dayanand S, Boppana SB, Auradi V, Nagaral M, Udaya Ravi M, Bharath, (2021) Evaluation of wear properties of heat-treated Al-AlB2 in-situ metal matrix composites. J Bio-and Tribo-Corrosion 7(2):40
5. Ali Z, Muthuraman V, Rathnakumar P, Gurusamy P, Nagaral M (2020) Investigation on the tribological properties of copper alloy reinforced with Gr/ZrO_2 particulates by stir casting route. Mater Today Proc 33:3449–3453
6. Prasad GP, Chittappa HC, Nagaral M, Auradi V (2020) Influence of B_4C reinforcement particles with varying sizes on the tensile failure and fractography of LM29 alloy composites. J Fail Anal Prev 20(6):2078–2086
7. Veerabhadrappa A, Hulipalled P, Lokesha V, Nagaral M, Auradi V (2022) Machine learning algorithms to predict wear behavior of modified ZA-27 alloy under varying operating parameters. J Bio-Tribo-Corros 8:1–10
8. Bharath V, Auradi V, Nagaral M, Bopanna SB (2020) Influence of alumina percentage on microstructure, mechanical and wear behavior of 2014 aluminium alumina metal matrix composites. Jurnal Tribologi 25(1):29–44
9. Vasanth Kumar HS, Kempaiah UN, Nagaral M, Auradi V (2021) Impact, tensile and fatigue failure analysis of boron carbide particles reinforced Al-Mg-Si (Al6061) alloy composites. J Fail Anal Prev 21(6):2177–2189
10. Murthy BV, Auradi V, Nagaral M, Vatnalmath M, Namdev N, Anjinappa C, Patil S, Razak A, Alsabhan AH, Alam S, Qamar MO (2023) Al2014–alumina aerospace composites: particle size impacts on microstructure, mechanical, fractography, and wear characteristics. ACS Omega 8(14):13444–13455
11. Shorowordi KM, Laoui T, Haseeb ASMA, Celis JP, Froyen L (2003) Microstructure and interface characteristics of B_4C, SiC and Al_2O_3 reinforced Al matrix composites: a comparative study. J Mater Process Technol 42(3):738–743
12. Shetty RP, Mahesh TS, Ali Z, Veeresha G, Nagaral M (2022) Studies on mechanical behaviour and tensile fractography of boron carbide particles reinforced Al8081 alloy advanced metal composites. Mater Today Proc 52:2115–2120
13. Somayaji A, Nagaral M, Anjinappa C, Alkahtani MQ, Billady RK, Kumar N, Auradi V, Islam S, Chowdary JRR, Razak A, Khan MA (2023) Influence of graphite particles on the mechanical and wear characterization of Al6082 alloy composites. ACS Omega 8(30):26828–26836
14. Raksha MS, Nagaral M, Boppana SB, Anjinappa C, Khan MS, Wahab MOA, Islam S, Bhardwaj V, Palavalasa RK, Khan MA, Razak A (2023) Impact of boron carbide particles and weight

percentage on the mechanical and wear characterization of Al2011 alloy metal composites. ACS Omega 8(26):23763–23771
15. Shetty RP, Raju TH, Nagaral M, Kumar N, Auradi V (2024) Effect of B_4C particles addition on the mechanical, tensile fracture and wear behavior of Al7075 alloy composites. J Bio- Tribo-Corros 10(2):32
16. Demir ME, Okumuş M (2024) Investigation of microhardness, microstructural, tribological, and thermal properties of Al7075/TiO2/kaoline hybrid metal matrix composites produced by powder metallurgy process. Adv Eng Mater 26(24):2401343. https://doi.org/10.1002/adem.202401343
17. Veeresha G, Manjunatha B, Bharath V, Nagaral M, Auradi V (2022) Synthesis, microstructural characterization, mechanical, fractographic and wear behavior of micro B_4C particles reinforced Al2618 alloy aerospace composites. Fract Struct Integr/Frattura ed Integrità Strutturale 62:385
18. Dharshan K, Raju TN, Nagaral M, Bharath V, Auradi V, Shantharaj P, Supreeth S (2022) Microstructure, tensile and impact behaviour of Si_3N_4 particles reinforced Al2024 matrix composites. Mater Today Proc 52:1499–1503
19. Raksha MS, Basavalingappa A, Nagaral M, Anjinappa C, Omprakash B, Razak A, Hasan N (2024) Impact of micro graphite particles addition on the mechanical behavior of Al2011 alloy metal composites. Eng Rep (Hoboken) 6(4):e12746
20. Kumar N, Kumar HV, Raju TH, Nagaral M, Auradi V, Veeresha RK (2022) Microstructural characterization, mechanical and taguchi wear behavior of micro-titanium carbide particle-reinforced Al2014 alloy composites synthesized by advanced two-stage casting method. J Bio-and Tribo-Corros 8(4):109
21. Kotresha Mydur, Mahendra Kumar, Madeva Nagaral, Virupaxi Auradi, V Bharath, TA Sudarshan. Microstructure, physical, tensile and wear behaviour of B_4C particles reinforced Al7010 alloy composites. Manufacturing Review, 10, 3, 2023.
22. Anjan Babu VA, Saravanan R, Raviprakash M, Nagaral M, Kumar N (2022) Microstructural characterization and wear behavior of 12 wt% of boron carbide reinforced Al2030 alloy composites. Mater Today Proc 52:439–444
23. Ali Z, Muthuraman V, Rathnakumar P, Gurusamy P, Nagaral M (2023) Influence of B_4C particle size on the mechanical behavior of A356 aluminium composites. Res Eng Struct Mater 9(2):527–540
24. R Murali Mohan, UN Kempaiah, B Manjunatha, Madeva Nagaral, V Auradi. Processing and wear behavior optimization of B_4C and rice husk ash dual particles reinforced ADC12 alloy composites using Taguchi method. Materials Physics & Mechanics, 50, 2, 2022.
25. Samuel Dayanand, S Manjunath Yadav, Madeva Nagaral, Satish Babu Boppana, TH Manjunatha, V Auradi. Influence of SiO_2 and nano graphene particles on the microstructure and mechanical behavior of A356 alloy metal composites. Research on Engineering Structures and Materials, 2024.
26. D Madhu, Shanawaz Patil, Madeva Nagaral, Samuel Dayanand, Chandrashekar Anjinappa, Ali Majdi, Abduljabar H Ali, Sameer Algburi, Abdul Razak. Synthesis and Tensile Characterisation of B_4C Particles Reinforced Al7475 (Al-Zn) Alloy Composites. Journal of Mines, Metals and Fuels, 2024, pp. 251–262.
27. Angadi SB, Kumar S, Nagaral M, Auradi V, Valukula B (2025) Effect of ceramic boron carbide particles addition on the mechanical and microstructural characteristics of Al7020 alloy composites. Mech Adv Compos Struct 12(1):169–218
28. Topcu I, Gulsoy HO, Kadigolu N, Gulluoglu AN (2009) Processing and mechanical properties of B_4C reinforced Al matrix composites. J Alloys Compd 48(1–2):516–521
29. Demir ME, Çelik YH, Kilickap E, Kalkanli A (2023) The effect of B4C reinforcements on the microstructure, mechanical properties, and wear behavior of AA7075 alloy matrix produced by squeeze casting. Proceedings of the Institution of Mechanical Engineers, Part E: Journal of Process Mechanical Engineering 237(6):2574–2584
30. Demir ME, Celik YH, Kalkanli A (2022) The effect of rolling and aging on mechanical and tribological properties in B_4C particle reinforced Al7075 matrix composites. Arab J Sci Eng 47:16187–16208
31. Subbaraya Mohan K, Namdev N, Konanur Vishwanathaiah M, Nagaral M, Kukanur V, Ali Z (2024) Mechanical properties and fractography of SiC and fly ash particulates reinforced Al2024 alloy aerospace metal composites. Braz J Develop 10(10):e73710–e73710
32. Juhany KA, Patil S, Pasha AA, Nagaral M (2024) Impact of T6 heat treatment on the microstructure and mechanical characterization of Al7075-graphene nanoplatelets-beryl hybrid composites. Interactions 245(1):311
33. Çelik YH, Demir ME, Kilickap E, Kalkanli A (2020) Investigation of wear behavior of aged and non-aged SiC-reinforced AlSi7Mg2 metal matrix composites in dry sliding conditions. J Braz Soc Mech Sci Eng 42(1):8
34. Ramachandra GS, Boppana SB, Dayanand S, Nagaral M, Singh AK (2024) Wear behavior of Si3N4 reinforced AA2219 metal matrix composites. J Mines Metals Fuels. https://doi.org/10.18311/jmmf/2024/4506
35. Dayanand S, Babu BS, Telagu A, Mukunda S, Singh AK, Nagaral M (2024) A review on carbon fiber reinforced metal matrix composites. J Mines Met Fuels 72:333–346
36. Chandrasekhar GL, Vijayakumar Y, Nagaral M, Rajesh A, Manjunath K, Kaviti RVP, Auradi V (2024) Synthesis and tensile behavior of Al7475-nano B_4C particles reinforced composites at elevated temperatures. Mater Phys Mech 52(3):44–57
37. Santosh V Janamatti, Raju Jadar, SB Angadi, Nagaraj Namdev, Subbaraya Mohan Kumar, Madeva Nagaral, AN Prashanth. Sliding Wear Characteristics of Zn-15Sn Alloy with Nano B_4C Reinforced Composites. Journal of Mines, Metals and Fuels,2024, 291–300.
38. VN Akanksh, Pranav Hegde, S Siddharth, AB Manjunath, C Siddaraju, Madeva Nagaral. Microstructural Characterization, Mechanical And Wear Behaviour Of Al2024-B_4C Composites For Aerospace Applications. Journal of Mines, Metals and Fuels, 2022, 138–142.
39. Bharath V, Auradi V, Nagaral M, Boppana SB, Ramesh S, Palanikumar K (2022) Microstructural and wear behavior of Al2014-alumina composites with varying alumina content. Trans Indian Inst Met. https://doi.org/10.1007/s12666-021-02405-4
40. Janamatti SV, Hunasikatti M, Venkatesh KC, Vijaykumar BP, Nagaral M, Auradi V (2024) Investigation on volumetric wear behaviour of Zn based metal composites with B_4C Reinforcement for sliding contact applications. Int J Veh Struct Syst 16(3):338–342
41. Bharat N, Akhil G, Bose PSC (2024) Metaheuristic approach to enhance wear characteristics of novel AA7178/nSiC metal matrix composites. J Mater Eng Perform 33:12638–12655
42. Bharat N, Bose PSC (2023) Optimizing the wear behaviour of AA7178 metal matrix composites reinforced with SiC and TiO_2 nanoparticles: a comparative study using evolutionary and statistical methods. SILICON 15:4703–4719